A calculation of phonon drag thermopower for a 2DEG subjected to an in-plane magnetic field

1992 J. Phys.: Condens. Matter 4 9041

(http://iopscience.iop.org/0953-8984/4/46/012)

J. Phys.: Condens. Matter 4 (1992) 9041–9052. Printed in the UK

A calculation of phonon drag thermopower for a 2DEG subjected to an in-plane magnetic field

H Tang and P N Butcher
Department of Physics, University of Warwick, Coventry CV4 7AL, UK

Received 6 July 1992, in final form 14 September 1992

Abstract. The phonon drag contribution S_{gxx} to the thermopower is calculated for a 2DEG by using Boltzmann equations for both electrons and phonons. The system has a parabolic confining potential and is subjected to an in-plane magnetic induction field $\boldsymbol{B}$ and the temperature gradient is parallel to $\boldsymbol{B}$. A quasi-phonon model is proposed which greatly simplifies the calculation of S_g. Qualitative comparison is made between the theoretical predictions and experimental data.

1. Introduction

In our previous work on 2DEGs [1], diffusion thermopower in the presence of elastic scattering has been considered for the case when subband depopulation is produced by a magnetic induction field $\boldsymbol{B}$ in the plane of the 2DEG. When the Fermi energy drops below the first excited subband the scattering rate suffers a sudden decrease which produces structure in the transport coefficients. Cantrell *et al* [2] have shown that the diffusion thermopower can change sign in these circumstances. Calculations [1, 3] and measurements [4, 5] have confirmed this behaviour.

A recent experiment by Fletcher *et al* [6] on a high-mobility GaAs/GaAlAs heterojunction has shown unexpected behaviour of the thermopower S as a function of B. Instead of the appearance of a valley or a change of sign in $-S$ the data exhibits a peak in $-S$ followed by a sharp fall near the depopulation field. The measurements were performed above 1 K. In that temperature range when $B = 0$ the phonon drag contribution to the thermopower can become dominant [7]. Fletcher *et al* [6] suggest that this is the origin of the difference between their experimental data and the results of the diffusion thermopower calculations.

In this paper, we use a Boltzmann equation approach to calculate the phonon drag thermopower S_{gxx} in a quasi-2D system subjected to a parabolic confining potential and an in-plane magnetic induction field $\boldsymbol{B}$. Attention is focused on the case when the temperature gradient is parallel to $\boldsymbol{B}$. The Boltzmann equations and their formal solutions for the electrons and phonons are given in the next section. In section 3, the symmetry of some quantities of interest and its use in simplifying the evaluation of the transport coefficients is discussed. We then introduce, in section 4, the 'phonon drag velocity' which plays a role in S_g which is analogous to that played by the electron velocity in diffusion thermopower. In section 5, we propose a 'quasi-phonon' model which greatly simplifies the calculations. The theoretical results are given and discussed in section 6. Finally, in section 7, we draw some conclusions.

0953-8984/92/469041+12$07.50

2. The Boltzmann equations for electrons and phonons

In the presence of an electric field E and a temperature gradient ∇T in the xy-plane, the linearized steady-state Boltzmann equations for the 2D electron and 3D phonon distribution functions are [1, 8]:

$$(\partial f_\alpha^1/\partial t)_c = (\mathrm{d}f_\alpha^0/\mathrm{d}\epsilon_\alpha)v_{e\alpha} \cdot [eE + (\epsilon_\alpha - \epsilon_F)\nabla T/T] \tag{1}$$

$$(\partial N_Q^1/\partial t)_c = -(\mathrm{d}N_Q^0/\mathrm{d}(\hbar\omega_Q))v_{pQ} \cdot \hbar\omega_Q \nabla T/T. \tag{2}$$

Here Q is the 3D acoustic phonon wave vector and $\alpha = \{n, k\}$, in which n is the subband index k is the 2DEG wave vector in the xy-plane.

Following Cantrell and Butcher [8] we take two collision mechanisms into account: elastic scattering and the electron–phonon interaction. The contribution to $(\partial f^1/\partial t)_c$ involving elastic scattering takes the form

$$\left(\frac{\partial f_\alpha^1}{\partial t}\right)_s = \sum_\beta (f_\beta^1 - f_\alpha^1)p^s(\alpha, \beta)$$

where $\beta = \{n', k'\}$. In this equation $p^s(\alpha, \beta)$ denotes a scattering rate. As discussed in [1, 2], it is not possible to simplify this equation within the relaxation time approximation because the parallel magnetic field makes the subband structure anisotropic. The contribution to $(\partial f_\alpha^1/\partial t)_c$ from the electron–phonon interaction is

$$\left(\frac{\partial f_\alpha^1}{\partial t}\right)_{ep} = \frac{1}{k_B T}\sum_{\beta Q}\left[\left(-\frac{\mathrm{d}f_\beta^0}{\mathrm{d}\epsilon_\beta}\right)^{-1} f_\beta^1 - \left(-\frac{\mathrm{d}f_\alpha^0}{\mathrm{d}\epsilon_\alpha}\right)^{-1} f_\alpha^1\right](\Gamma_{\alpha\beta}^Q + \Gamma_{\beta\alpha}^Q)$$

$$+ \frac{1}{k_B T}\sum_{\beta Q}\left(-\frac{\mathrm{d}N_Q^0}{\mathrm{d}(\hbar\omega_Q)}\right)^{-1} N_Q^1(\Gamma_{\alpha\beta}^Q - \Gamma_{\beta\alpha}^Q)$$

where

$$\Gamma_{\alpha\beta}^Q = f_\alpha^0(1 - f_\beta^0)p^{e0}(\alpha, \beta; Q) \qquad \Gamma_{\beta\alpha}^Q = f_\alpha^0(1 - f_\beta^0)p^{a0}(\alpha, \beta; Q)$$

are equilibrium electron fluxes from α to β involving phonon emission and phonon absorption respectively. The reader is referred to [8] for expressions for $p^{e0}(\alpha, \beta; Q)$ and $p^{a0}(\alpha, \beta; Q)$.

The first term in $(\partial f_\alpha^1/\partial t)_{ep}$ can be neglected in comparison with the elastic scattering contribution $(\partial f_\alpha^1/\partial t)_s$ to $(\partial f_\alpha^1/\partial t)_c$. Then we have

$$\left(\frac{\partial f_\alpha^1}{\partial t}\right)_c = \sum_{\beta Q}(f_\beta^1 - f_\alpha^1)p^s(\alpha, \beta) + \frac{1}{k_B T}\sum_{\beta Q}\left(-\frac{\mathrm{d}N_Q^0}{\mathrm{d}(\hbar\omega_Q)}\right)^{-1} N_Q^1(\Gamma_{\alpha\beta}^Q - \Gamma_{\beta\alpha}^Q). \tag{3}$$

At liquid helium temperatures the phonon relaxation is dominated by boundary scattering for which a relaxation time approximation *is* valid (the magnetic field has no effect on the phonons). Moreover, the contribution from the electron–phonon

interaction to $(\partial N_{\boldsymbol{Q}}^1/\partial t)_c$ can be omitted because it contributes only in second order to f_α^1. Hence, for phonons we have simply

$$(\partial N_{\boldsymbol{Q}}^1/\partial t)_c = -N_{\boldsymbol{Q}}^1/\tau_p \tag{4}$$

where τ_p is the phonon relaxation time.

We define the electron lifetime as

$$\tau_0(\alpha) = \left[\sum_\beta p^s(\alpha,\beta)\right]^{-1}. \tag{5}$$

Then we may substitute $N_{\boldsymbol{Q}}^1$ from (4) into (3) and, using (1) and (2), obtain the equation

$$f_\alpha^1 = \tau_0(\alpha)\frac{df_\alpha^0}{d\epsilon_\alpha}\boldsymbol{v}_{e\alpha}\cdot\left[e\boldsymbol{E} + (\epsilon_\alpha - \epsilon_F)\frac{\nabla T}{T}\right] - \tau_0(\alpha)\frac{1}{k_B T}$$
$$\times \sum_{\beta\boldsymbol{Q}} \tau_p(\Gamma_{\alpha\beta}^{\boldsymbol{Q}} - \Gamma_{\beta\alpha}^{\boldsymbol{Q}})\boldsymbol{v}_{p\boldsymbol{Q}}\cdot\hbar\omega_{\boldsymbol{Q}}\frac{\nabla T}{T} + \tau_0(\alpha)\sum_\beta f_\beta^1 p^s(\alpha,\beta) \tag{6}$$

from which to determine f_α^1.

As in reference [1], it is convenient to introduce the 'renormalized electron velocity' $\boldsymbol{V}_e(\alpha)$ which is defined by the equation

$$\boldsymbol{V}_e(\alpha) = \boldsymbol{v}_{e\alpha} + \sum_\beta p^s(\alpha,\beta)\tau_0(\beta)\boldsymbol{V}_e(\beta). \tag{7}$$

It is also convenient in the present calculation to introduce the 'phonon drag velocity' $\boldsymbol{V}_g(\alpha)$ by means of the analogous equation

$$\boldsymbol{V}_g(\alpha) = \boldsymbol{V}_{g0}(\alpha) + \sum_\beta p^s(\alpha,\beta)\tau_0(\beta)\boldsymbol{V}_g(\beta) \tag{8}$$

where

$$\boldsymbol{V}_{g0}(\alpha) = \frac{-1}{k_B T}\sum_{\beta\boldsymbol{Q}} \tau_p(\Gamma_{\alpha\beta}^{\boldsymbol{Q}} - \Gamma_{\beta\alpha}^{\boldsymbol{Q}})\hbar\omega_{\boldsymbol{Q}}\boldsymbol{v}_{p\boldsymbol{Q}}. \tag{9}$$

Then f_α^1 can be written in the superficially simple form

$$f_\alpha^1 = \tau_0(\alpha)\frac{df_\alpha^0}{d\epsilon_\alpha}\boldsymbol{V}_e(\alpha)\cdot\left[e\boldsymbol{E} + (\epsilon_\alpha - \epsilon_F)\frac{\nabla T}{T}\right] + \tau_0(\alpha)\boldsymbol{V}_g(\alpha)\cdot\frac{\nabla T}{T}. \tag{10}$$

3. The symmetry of the transport coefficients

The transport coefficients σ_{ij} and L_{ij} are defined in [9] by

$$J_i = -\frac{e}{A}\sum_\alpha f_\alpha^1 v_{e\alpha i} = \sum_j [\sigma_{ij} E_j + L_{ij}(\nabla T)_j] \tag{11}$$

where A is the area of the 2DEG. Substituting (10) in (11) we see that

$$\sigma_{ij} = -\frac{e^2}{A}\sum_\alpha \tau_0(\alpha)\left(\frac{\mathrm{d}f_\alpha^0}{\mathrm{d}\epsilon_\alpha}\right) v_{e\alpha i} V_{ej}(\alpha) \tag{12}$$

and

$$L_{ij} = -\frac{e}{AT}\sum_\alpha \tau_0(\alpha)\left(\frac{\mathrm{d}f_\alpha^0}{\mathrm{d}\epsilon_\alpha}\right)(\epsilon_\alpha - \epsilon_F) v_{e\alpha i} V_{ej}(\alpha) - \frac{e}{AT}\sum_\alpha \tau_0(\alpha) v_{e\alpha i} V_{gj}(\alpha). \tag{13}$$

The first term in the right-hand side of (13) is independent of the electron–phonon interaction. It is the 'diffusion' term which we denote by L_{dij}. The second term is due to phonon drag and is our main concern. We denote it by L_{gij}.

To simplify the calculation of L_{dij} and L_{gij} we assume, as in [1], a parabolic confining potential and put $B = (B, 0, 0)$. We also suppose that the elastic scattering is caused by randomly located δ-function potentials. The electron–phonon interaction is written in the isotropic form

$$H_{ep} = E_1 \nabla \cdot \boldsymbol{u} \tag{14}$$

where E_1 is the deformation potential and the 3D lattice displacement $\boldsymbol{u}$ has the standard form [8]:

$$\boldsymbol{u} = \sum_{\boldsymbol{Q}} \left(\frac{\hbar}{2\rho V \omega_{\boldsymbol{Q}}}\right)^{1/2} \eta_{\boldsymbol{Q}} \cdot \boldsymbol{Q}(\alpha_{\boldsymbol{Q}}^+ \mathrm{e}^{-\mathrm{i}\boldsymbol{Q}\cdot\boldsymbol{R}} + \alpha_{\boldsymbol{Q}} \mathrm{e}^{\mathrm{i}\boldsymbol{Q}\cdot\boldsymbol{R}}).$$

where $\eta_{\boldsymbol{Q}}$ is a polarization vector and $\alpha_{\boldsymbol{Q}}^+$ and $\alpha_{\boldsymbol{Q}}$ are creation and annihilation operators.

In [1] we discuss the symmetry of the interband elastic scattering rates and the corresponding electron lifetimes. We show there that these symmetries lead to the following results for the renormalized electron velocity

$$V_{ex}(\alpha) = v_{e\alpha x} \tag{15a}$$

$$V_{ey}(n, k_x, k_y) = V_{ey}(n, -k_x, k_y) = -V_{ey}(n, k_x, -k_y). \tag{15b}$$

We also show in [1] that, as a consequence of (15) $[\sigma_{ij}]$ and $[L_{ij}]$ are diagonal matrices in the absence of phonons.

It is not difficult to generalize the above arguments to deal with the model under discussion here which includes the electron–phonon interaction. The electron

transition rates produced by this interaction when a phonon of wavevector Q is either absorbed or emitted are given in [8]. To determine the symmetry of the zero-order phonon drag velocity $V_{g0}(\alpha)$ in (9) we change the signs of k_x (or k_y) for state α and k'_x (or k'_y) for state β and q_x (or q_y) in the phonon wavevector. These changes preserve both energy and momentum conservation. Using the formulae in [8] we then find that the factor multiplying the phonon velocity v_{pQ} in (9) is invariant, while in v_{pQ} itself either the x (or y) component changes sign. It follows that

$$V_{g0x}(n,k_x,k_y) = V_{g0x}(n,k_x,-k_y) = -V_{g0x}(n,-k_x,k_y) \tag{16a}$$

$$V_{g0y}(n,k_x,k_y) = V_{g0y}(n,-k_x,k_y) = -V_{g0y}(n,k_x,-k_y). \tag{16b}$$

We note that (15a) implies that $V_{ex}(\alpha)$ has the same symmetry in k space as $V_{g0x}(n,k_x,k_y)$ which is exhibited in (16a).

Proceeding as in [1] we find that (15) and (16) yield the following results for the renormalized phonon drag velocity:

$$V_{gx}(\alpha) = V_{g0x}(\alpha) \tag{17a}$$

$$V_{gy}(n,k_x,k_y) = V_{gy}(n,-k_x,k_y) = -V_{gy}(n,k_x,-k_y). \tag{17b}$$

Equations (17) are completely analogous to equations (15). Taken together, (15) and (17) imply that the matrices $[\sigma_{ij}]$ and $[L_{ij}]$ remain diagonal in the presence of phonons. Hence the total thermopower tensor is also diagonal with elements

$$S_{xx} = -L_{xx}/\sigma_{xx} \qquad S_{yy} = -L_{yy}/\sigma_{yy}. \tag{18}$$

Moreover, if we confine our attention to σ_{xx} and S_{xx}, we only need $v_{e\alpha x}$ and $V_{g0x}(\alpha)$ which are given explicitly by equations (21b) and (9) respectively. We confine our attention to this simple case in the calculations which follow. In [1] we calculate $V_{ey}(\alpha)$ iteratively from (7) and use the result to evaluate σ_{yy} and the diffusion thermopower tensor element S_{dyy} in the absence of phonons. Phonon drag has a negligible effect on σ_{yy} but it determines the phonon drag thermopower tensor element S_{gyy} which is important in GaAs/GaAlGaAs heterojunctions above 1 K. We will discuss the iterative solution of (8) for $V_{gy}(\alpha)$ and its application to the calculation of S_{gyy} in another paper.

4. The phonon drag velocity

The contribution to L_{xx} in (13) involving $V_{ex}(\alpha)$ has a significant factor $\mathrm{d}f^0_\alpha/\mathrm{d}\epsilon_\alpha$ in the summand. It is useful to pull the same factor out of the summand of the contribution to L_{xx} involving $V_{g0}(\alpha)$. To do so we use the identities

$$f^0_\alpha(1-f^0_\beta)(N^0_Q+1) = -k_B T(\mathrm{d}f^0_\alpha/\mathrm{d}\epsilon_\alpha)(1-f^0_\beta+N^0_Q) \tag{19a}$$

$$f^0_\alpha(1-f^0_\beta)N^0_Q = -k_B T(\mathrm{d}f^0_\alpha/\mathrm{d}\epsilon_\alpha)(f^0_\beta+N^0_Q) \tag{19b}$$

which are valid when $\epsilon_\beta = \epsilon_\alpha - \hbar\omega_Q$ in (19a) and when $\epsilon_\beta = \epsilon_\alpha + \hbar\omega_Q$ in (19b). These conditions are imposed by the energy-conserving δ-functions which multiply these two expressions in $V_{g0x}(\alpha)$. We may use (19) to write

$$V_{g0}(\alpha) = (\mathrm{d}f^0_\alpha/\mathrm{d}\epsilon_\alpha)U_{g0}(\alpha) \tag{20}$$

in which $U_{g0}(\alpha)$ is easily identified.

For a parabolic confining potential $V(z) = m^*\omega_0^2 z^2/2$ the electron energy and velocity are [1]

$$\epsilon_\alpha = (\hbar^2/2m^*)k_x^2 + (\hbar^2/2m_y^*)k_y^2 + (n + \tfrac{1}{2})\hbar\omega_c \tag{21a}$$

$$v_{e\alpha} = (\hbar k_x/m^*, \hbar k_y/m_y^*) \tag{21b}$$

where m^* is the effective mass of the electrons and m_y^* is given by

$$m^*/m_y^* \equiv \gamma = (\omega_0/\omega)^2 \tag{22}$$

with $\omega^2 = \omega_0^2 + \omega_c^2$ in which ω_c is the cyclotron frequency.

It is useful to introduce the 2D wavevector $\boldsymbol{k}^* = (k_x, \sqrt{\gamma}k_y)$. Then ϵ_α is fixed by the magnitude of $\boldsymbol{k}^*$ and $v_{e\alpha x}$ and $v_{e\alpha y}$ are respectively proportional to $\cos\theta$ and $\sin\theta$ where θ is the angle between $\boldsymbol{k}^*$ and the x-axis. We also find that the calculated θ-dependences of $U_{g0x}(\alpha)$ and $U_{g0y}(\alpha)$ for various subbands and various parameter values are approximately proportional to $\cos\theta$ and $\sin\theta$ respectively. To exploit this simple behaviour we introduce a three-point approximation:

$$U_{g0x}(\theta) = \cos\theta\left\{U_{g0x}(\theta = 0) - 2\left[U_{g0x}(\theta = 0) - \sqrt{2}U_{g0x}(\theta = \pi/4)\right]\sin^2\theta\right\}$$

$$U_{g0y}(\theta) = \sin\theta\left\{U_{g0y}(\theta = \pi/2) + (2/\sqrt{\gamma})\right.$$
$$\left.\times\left[U_{g0x}(\theta = 0) - \sqrt{2}U_{g0x}(\theta = \pi/4)\right]\cos^2\theta\right\}. \tag{23}$$

In figure 1 the solid lines show exact values of U_{g0x} and U_{g0y} when $n/n_0 = 2.37$ and the dots and crosses are derived from (23). Here, n is the electron density and $n_0 = m^*\omega_0/h$ is a characteristic electron density for our model [1]. It can be seen from the figure that the approximation (23) is reasonable. When $B = 0$, U_{g0x} and U_{g0y} have exact $\cos\theta$ and $\sin\theta$ variations when k is fixed. This is easy to understand physically. As a consequence of momentum conservation the phonon velocity is proportional to $\boldsymbol{k} - \boldsymbol{k}'$. After the summation over $\boldsymbol{k}'$, only the component of $\boldsymbol{k} - \boldsymbol{k}'$ which is parallel to $\boldsymbol{k}$ makes a contribution to $U_{g0}(\alpha)$ because the system is isotropic when $B = 0$. Hence the θ-dependence of U_{g0} is the same as that of $\boldsymbol{k}$.

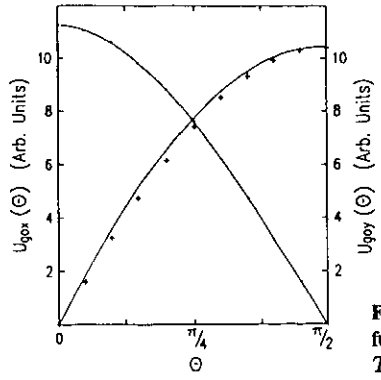

Figure 1. $U_{g0x}(\alpha)$ in the ground subband as a function of the angle θ when $\epsilon_\alpha = 19.385$ meV, $T = 1.5$ K, $B = 4.28$ T and $n/n_0 = 2.37$.

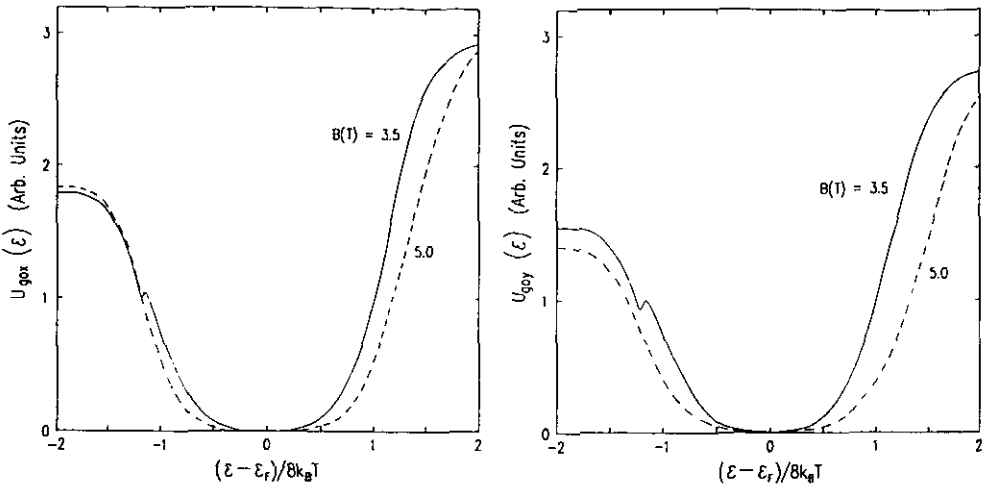

Figure 2. Left-hand panel: $U_{g0x}(\alpha)$ as a function of the energy ϵ_α in the ground subband when $\theta = 0$ and $B = 3.5$ and 5 T, $T = 1.5$ K and $n/n_0 = 2.37$. Right-hand panel: $U_{g0y}(\alpha)$ as a function of the energy ϵ_α in the first subband when $\theta = \pi/2$ and $B = 3.5$ and 5 T, $T = 1.5$ K and $n/n_0 = 2.37$.

Figure 2 shows the energy dependence of U_{g0x} and U_{g0y} when ϵ_α is near the Fermi energy. Both quantities take minimum values near ϵ_F. From (19) we know that there is a factor $1-f^0_\beta \cong 1-f^0(\epsilon_\alpha-\hbar\omega_Q)$ involved in the phonon emission process which is most important when $\epsilon_\alpha > \epsilon_F+\hbar\omega_Q$. Similarly, the factor $f^0_\beta = f^0(\epsilon_\alpha+\hbar\omega_Q)$ which is involved in the phonon absorption process is most important when $\epsilon_\alpha < \epsilon_F-\hbar\omega_Q$. Consequently, for electron energies near ϵ_F the sum of these two processes yields small values of both U_{g0x} and U_{g0y}. The factor $(\mathrm{d}f^0_\alpha/\mathrm{d}\epsilon_\alpha)$ in (20) has a peak at the Fermi energy with a half width $1.8k_BT$. It is usually set equal to a δ-function at low temperatures. We do not make that approximation here because the behaviour of U_{g0} described above gives a significant width to the peak in the components of V_{g0} at the Fermi level. The broadening effect is especially strong when the Fermi energy is located near a subband edge and must be allowed for in the calculations.

5. The quasi-phonon model

In this section we develop a useful approximation to $U_{g0}(\alpha) = V_{g0}/(\mathrm{d}f^0_\alpha/\mathrm{d}\epsilon_\alpha)$ which simplifies the summation over all possible phonon modes in (9). Inspection of figure 2 (left hand panel) shows that $U_{g0x}(\alpha)$ looks like $1 - f^0(\epsilon_\alpha - \hbar\omega_{Q^*})$ when $\epsilon_\alpha > \epsilon_F$ and it looks like $f^0(\epsilon_\alpha + \hbar\omega_{Q^*})$ when $\epsilon_\alpha < \epsilon_F$ where Q^* (which is different in the two cases) is fixed. Thus the behaviour is what we would expect if one phonon with a characteristic wave number Q^* dominated the absorption process and another phonon with a different Q^* dominated the emission process. To exploit this observation we introduce a modified temperature T^*_1, a modified Fermi energy ϵ^*_{F1} and a characteristic wave number Q^*_1 when $\epsilon_\alpha > \epsilon_F$ and similar quantities T^*_2, ϵ^*_{F2} and Q^*_2 when $\epsilon_\alpha < \epsilon_F$. Then we use the approximations

$$U_{g0x}(\epsilon_\alpha) = U_{01}\left\{\left[\exp\left(\frac{\hbar v_s Q_1^*}{k_B T_1^*}\right)-1\right]^{-1}+\left[\exp\left(\frac{\hbar v_s Q_1^*+\epsilon_{F1}^*-\epsilon_\alpha}{k_B T_1^*}\right)+1\right]^{-1}\right\}$$

$$\epsilon_\alpha > \epsilon_F$$

$$= U_{02}\left\{\left[\exp\left(\frac{\hbar v_s Q_2^*}{k_B T_2^*}\right)-1\right]^{-1}+\left[\exp\left(\frac{\hbar v_s Q_2^*-\epsilon_{F2}^*+\epsilon_\alpha}{k_B T_2^*}\right)+1\right]^{-1}\right\}$$

$$\epsilon_\alpha < \epsilon_F. \tag{24}$$

The parameters in (24) can be determined by calculating $U_{g0x}(\alpha)$ at a few points. When $B < 9$ T the error in this approximation is usually less than 5%. When ϵ_F is near the subband edge, it goes up to $\sim 8\%$ in some cases. Calculations also show that T^* and ϵ_F^* are not far from the actual values of T and ϵ_F. Consequently, the basic idea of using a characteristic wavenumber to simulate the whole process does not change the theoretical description in a significant way. We give some typical results of this approximation when $T = 1.05$ K and $n/n_0 = 3$ in table 1. The parameters in (24) are obtained from exact four-point calculation of U_{g0x}. The depopulation field B_c in this case is about 7.4 T around which Q^* shows an obvious decrease which reflects the disappearance of the inter-subband emission and absorption scattering processes. In the right hand panel of figure 2 we show U_{g0y} which may be approximated in the same way.

Table 1. The fitting parameters T_1^*, T_2^*, ϵ_{F1}^*, ϵ_{F2}^*, Q_1^* and Q_2^* used in the quasi-phonon model for the ground subband when $\theta = 0$, $T = 1.05$ K and $n/n_0 = 3.0$.

B (T)	T_1^* (K)	T_2^* (K)	ϵ_F (meV)	ϵ_{F1}^* (meV)	ϵ_{F2}^* (meV)	$\hbar V_s Q_1^*$ (meV)	$\hbar V_s Q_2^*$ (meV)
0	1.09	1.05	31.4	31.5	31.3	0.458	0.418
1	1.09	1.05	31.4	31.5	31.3	0.462	0.418
2	1.09	1.04	31.4	31.5	31.3	0.465	0.418
3	1.09	1.04	31.6	31.7	31.5	0.465	0.419
4	1.09	1.04	31.7	31.8	31.6	0.473	0.423
5	1.09	1.04	32.0	32.1	31.9	0.483	0.430
6	1.09	1.04	32.3	32.4	32.2	0.492	0.438
7.4	1.11	1.05	32.9	33.0	32.8	0.414	0.396
8	1.15	1.07	32.6	32.7	32.5	0.453	0.398

6. Results and analysis

To compare the theoretical results with the data of Fletcher *et al* [6], we use the GaAs effective mass $m^* = 0.067m_e$ and material density $\rho = 5.3 \times 10^3$ kg m^{-3}; we also set the acoustic phonon velocity $V_s = 5.1 \times 10^3$ m s^{-1} and the deformation potential $E_1 = 8$ eV [8]. The critical electron density at which ϵ_F enters the first excited subband in the experiment is in the order of 5×10^{15} m^{-2} [6]. Using this value we find that the characteristic electron density $n_0 = m^*\omega_0/h$ is in the order of 2.5×10^{15} m^{-2}. Hence $\hbar\omega_0 = 17.92$ meV. We find that reasonable values of resistance and phonon drag thermopower can be obtained by setting τ_0 [1] and the

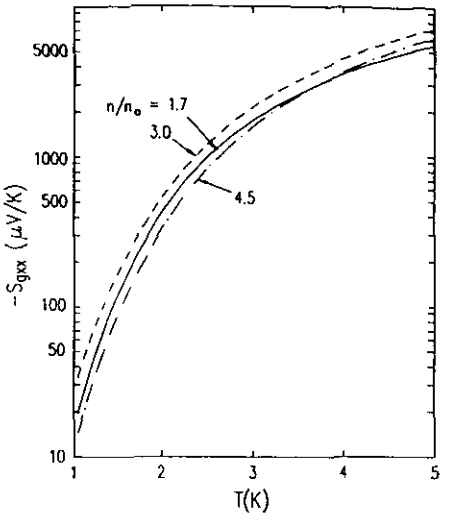

Figure 3. The dependence of phonon drag thermopower S_{gxx} on temperature T when $B = 0$ and $n/n_0 = 1.17$ (solid line), 3.0 (dashed line) and 4.5 (dash-dot line).

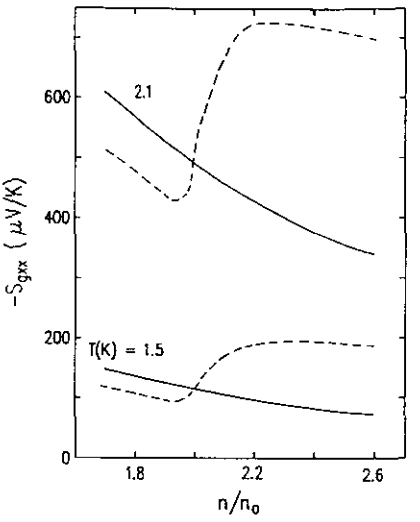

Figure 4. The dependence of phonon drag thermopower S_{gxx} on the electron density when $T = 1.5$ and 2.1 K and $B = 0$ (dashed lines) and 6 T (solid lines).

phonon relaxation time τ_p equal to 400 ps and 6×10^5 ps respectively. In the present calculations we neglect the energy dependence of the electron lifetime within one subband which is a good approximation when $\hbar\omega_0 \sim 18$ meV [1].

The phonon drag thermopower as a function of T at $B = 0$ and as a function of n/n_0 when $B = 0$ and 6 T are shown in figures 3 and 4 respectively. The results are qualitatively consistent with experiment [6]. Quantitatively the theoretical curves change more rapidly as T increases and, when the Fermi level passes into the first excited subband, the calculated sudden rise of thermopower is much larger than is seen experimentally. These differences can be understood by considering the following points. Firstly, we use a constant phonon relaxation time whereas in reality it is temperature dependent. Secondly, the theoretical relation between ϵ_F and n is unrealistic because we use a simple parabolic confining potential. Thirdly, energy-level broadening effects have been ignored altogether in the calculation.

The phonon drag thermopower $-S_{gxx}$ as the function of B at various values of n/n_0 when $T = 1.05$ K and 1.5 K is shown in figures 5 and 6 respectively. Resistivity results at $T = 1.5$ K are presented in figure 7 for comparison. As in the experiments [6], structure appears in the plot of $-S_{gxx}$ against B when n/n_0 exceeds a certain value. When $n/n_0 = 3$, for example, $-S_{gxx}$ initially rises and then falls sharply near the depopulation field. Figure 8 shows the temperature dependence of plots of $-S_{gxx}$ against B. As would be expected, the shallow peak structure gradually disappears with increasing temperature in agreement with the data. By comparing figures 6 and 7 we confirm that the peak structure of $-S_{gxx}$ is not due to the increase of resistivity alone. When n/n_0 is 2.2 or 2.5, the resistivity has a peak but the phonon drag thermopower does not.

The experimental peak of $-S_{gxx}$ is much sharper than we calculate. The most likely explanation is that the calculations are made with E parallel to B and the measurements are made with E perpendicular to B. In our model, a sharp drop

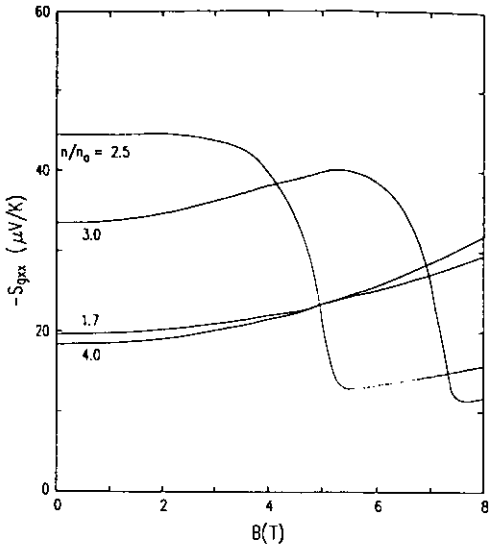

Figure 5. Phonon drag thermopower S_{gxx} as a function of B at $T = 1.05$ K with n/n_0 as indicated on the curves.

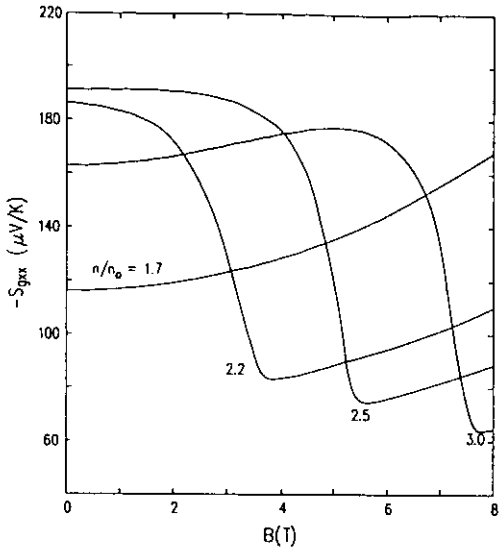

Figure 6. Phonon drag thermopower S_{gxx} as a function of B at $T = 1.5$ K with n/n_0 as indicated on the curves.

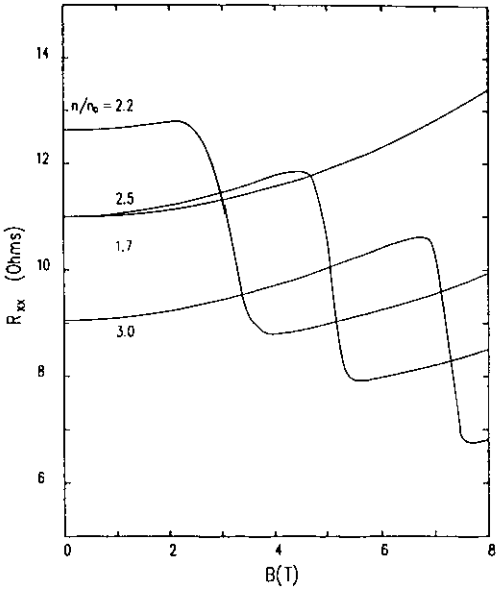

Figure 7. Resistivity R_{xx} as a function of B at $T = 1.5$ K with n/n_0 as indicated on the curves.

of the $-S_{gxx}$ near the depopulation field B_c is caused by the disappearance of the inter-subband emission and absorption scattering processes when the Fermi energy drops below the bottom of the first excited subband. The theoretical origin of the increase of $-S_{gxx}$ in the region of $B < B_c$ is that a phonon mode with a larger effective Q is involved as B increases for both inter- and intra-subband scattering processes. We would expect the primary effect of this to be similar in S_{gxx} and S_{gyy}. However, the parallel component of the phonon drag velocity component $V_{g0x}(\epsilon_F)$

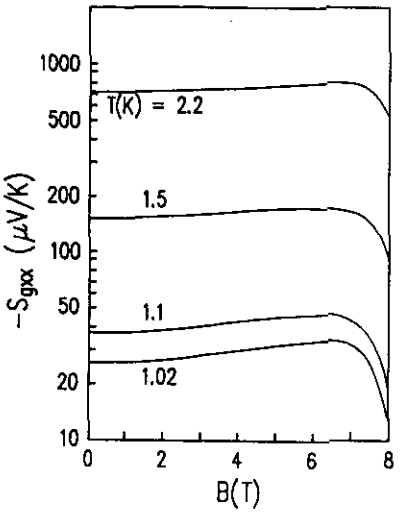

Figure 8. Phonon drag thermopower S_{gxx} as a function of B at $n/n_0 = 3.2$ with T as indicated on the curves.

shows a monotonic decrease with B which greatly depresses the peak of $-S_{gxx}$, and even suppresses the peak altogether when $n/n_0 < 2.5$. Numerical comparison of the values of $U_{g0x}(\epsilon_F)$ and $U_{g0y}(\epsilon_F)$ given in figures 2.1 and 2.2 (which are too small to be identified directly from the figures) show that $U_{g0y}(\epsilon_F)$ is larger than $U_{g0x}(\epsilon_F)$ in value, and that it also has a positive slope when B increases. Iterative calculations of $U_{gy}(\epsilon_F)$ are needed to see if this behaviour is maintained sufficiently strongly in higher orders to secure agreement with the experimental data.

7. Conclusion

We have presented the results of calculations of the element S_{gxx} of the phonon drag thermopower tensor when an in-plane magnetic field is applied to a 2DEG in the x-direction. The theory predicts that S_{gxx} will increase sharply with electron density when the Fermi level enters the first excited subband. It also shows that, for some electron densities, S_{gxx} increases (rather gently) with B as a depopulation field is approached after which it decreases sharply. Measurements have been made of S_{gyy} which shows behaviour which is qualitatively similar to that calculated for S_{gxx}. However, the experimental results are less sensitive to n and more sensitive to B. Calculations of S_{gyy} are required but they necessitate iterative solution of an equation for the y-component of the phonon drag velocity V_{gy}. In zeroth order V_{gy} behaves in a way which suggests that a calculation of S_{gyy} will yield behaviour in much better agreement with the experimental data. If these indications are preserved in higher orders of iteration then it would be worthwhile to calculate S_{gyy} for a realistic confining potential and more realistic scattering mechanisms.

References

[1] Tang H and Butcher P N 1988 *J. Phys. C: Solid State Phys.* **21** 3313
[2] Cantrell D G and Butcher P N 1985 *J. Phys. C: Solid State Phys.* **18** L587
[3] Cantrell D G and Butcher P N 1985 *J. Phys. C: Solid State Phys.* **18** 6639

[4] Ruf C, Brummell M A, Gmelin E and Ploog K 1989 *Superlatt. Microstruct.* **6** 175
[5] Nicholas R J, Nasir F and Singleton J 1988 *J. Cryst. Growth* **86** 656
[6] Fletcher R, Harris J J and Foxon C T 1991 *Semicond. Sci. Technol.* **6** 54
[7] Fletcher R, D'Iorio M, Sachrajda A S, Stoner R, Foxon C T and Harris J J 1988 *Phys. Rev.* B **37** 3137
[8] Cantrell D G and Butcher P N 1987 *J. Phys. C: Solid State Phys.* **20** 1985
[9] Butcher P N 1973 *Electrons on Crystalline Solids* ed A Salam (Vienna: IAEA)